

Tight-binding Hamiltonian for LaOFeAs

D.A. Papaconstantopoulos

Department of Computational and Data Sciences, George Mason University, Fairfax VA 22030

M.J. Mehl

Center for Computational Materials Science, Naval Research Laboratory, Washington DC 20375

M.D. Johannes

Center for Computational Materials Science, Naval Research Laboratory, Washington, DC 20375

(Dated: Printed on November 2, 2018)

First-principles electronic structure calculations have been very useful in understanding some of the properties of the new iron-based superconductors. Further explorations of the role of the individual atomic orbitals in explaining various aspects of research in these materials, including experimental work, would benefit from the availability of a tight-binding(TB) Hamiltonian that accurately reproduces the first-principles band structure results. In this work we have used the NRL-TB method to construct a TB Hamiltonian from Linearized Augmented Plane Wave(LAPW) results. Our TB model includes the Fe d-orbitals, and the p-orbitals from both As and O for the prototype material LaOFeAs. The resulting TB band structure agrees well with that of the LAPW calculations from 2.7 eV below to 0.8 eV above the Fermi level, ε_F , and the Fermi surface matches perfectly to that of the LAPW. The TB densities of states(DOS) are also in very good agreement with those from the LAPW in the above energy range, including the per orbital decomposition. We use our results to provide insights on the existence of a pseudogap in the DOS just above the Fermi level. We have also performed a separate TB fit to a database of LAPW results as a function of volume and with variations of the As positions. This fit although less accurate regarding the band structure near ε_F , reproduces the LAPW total energies very well and has transferability to non-fitted energies.

I. INTRODUCTION

The discovery of superconductivity with critical temperature T_c of about 55K in the iron compounds named iron-Oxypnictides^{1,2} has brought to the field excitement comparable to that created by the high T_c cuprates. The prototype formula for these materials is LaOFeAs with two distinct layers of LaO and FeAs. The room-temperature crystal structure is tetragonal and undergoes a structural distortion to orthorhombic at low temperatures³. The transition temperature is modulated by electron doping (F substituting for O)¹ or hole doping (Sr substituting for La)⁴. Other substitutions may occur, *e.g.*, replacing Fe by Ni⁵ or As by P⁶.

Many experimental and theoretical investigations have been performed without reaching a consensus as to whether these materials are similar to the cuprates, with their superconducting mechanism not yet understood, or if the essential physics is different, indicating that this is yet another class of superconductors. Questions to be answered include the nature of the normal state, the symmetry of the superconducting state and, of course, the origin of the pairing interaction.

Density functional theory (DFT) calculations^{7,8} have been at the center of the theoretical investigations. For LaOFeAs, Singh and Du⁹ found a high density of states at the Fermi level, $N(\varepsilon_F)$, and a low carrier concentration. We note that this is different from the cuprates which have a low $N(\varepsilon_F)$ and while displaying low carrier concentrations they are characterized by a half-filled

band near ε_F . On the other hand, Singh and Du found a high $N(\varepsilon_F)$ with antiferromagnetic fluctuations, which has a definite similarity with the cuprates. On the same theme, competing antiferromagnetism and superconductivity in the doped system is suggested by Yildirim¹⁰ as breaking the tetragonal symmetry causing a structural distortion.

Since standard DFT is very expensive computationally there is a need for developing tight-binding (TB) models that can be the starting point for carrying out further investigations using many-body techniques, such as multiband Hubbard models. Having examined the details of the DFT calculations for LaOFeAs, we identified the following features of the energy bands emerging from a wave function analysis. Starting from the lower bands we find O p-states that, for higher energies, hybridize with As p-states. Hybridization with Fe d-states occurs at the top of the As p-states and then hybridization with La states appears high above the Fermi level. Therefore, it becomes clear that TB models that ignore the other elements and use only the Fe d-orbitals are not reproducing the band structure of LaOFeAs accurately enough.

Several TB approaches have appeared in the literature, such as the study of Kuroki *et al.*¹¹, which is based on an Fe-only d-band Hamiltonian. These authors applied the random phase approximation to obtain spin and charge susceptibilities, concluding that an unconventional s-wave pairing is in play. Furthermore, a recent paper by Manousakis *et al.*¹² builds a TB Hamiltonian fitted to DFT results using in addition to the Fe

d-orbitals p orbitals of As. Based on their TB Hamiltonian these authors report that the effective Hamiltonian, in the strong on-site Coulomb-repulsion limit, operates on three distinct subspaces coupled through Hund's rule. They also argue that the observed spin-density-wave order minimizes the ground state energy of the Hamiltonian. These conclusions could be a correct speculation of the physics in this material. However, their calculations are based on a TB Hamiltonian that is not accurately derived from the first-principles data. Although they performed their TB fit only near the Fermi level, their results do not reproduce the energy bands well enough, as can be seen in their Fig 4. Therefore, the conclusions of this paper, based on a poorly constructed TB Hamiltonian, can only be considered as a speculation. More recently a paper by Eschrig and Koepf¹³ presents a minimal basis TB Hamiltonian for LaOFeAs, as well as for other structure types of the Fe superconductors, that is based on an elegant TB theory. However, this Hamiltonian has quantitative agreement to first-principles results only in a smaller window around E_F than the fit we present here.

There are two other 5-orbital tight-binding studies with which we compare in our results section. These are the work of Calderón *et al.*¹⁴ and Graser *et al.*¹⁵

In this work we have used the Naval Research Laboratory Tight-Binding (NRL-TB)^{16,17} method to fit our linearized augmented plane wave (LAPW) results^{18–20} to a TB basis with the aim of reproducing the band structure very accurately. We have included the d orbitals of Fe, the p orbitals of As, and the p orbitals of O, leaving out the La orbitals since their effect is only evident high above ε_F . In this study we examine the effect of each of the above orbitals on how accurately the first-principles band structure can be reproduced.

In this work we fit the NRL-TB method to an LAPW band structure ranging from 2.7 eV below to 0.8 eV above ε_F . The TB band structure fits the LAPW results very well near ε_F and perfectly reproduces the Fermi surface near the Γ and M symmetry points.

The TB densities of states are also in very good agreement with the corresponding LAPW results, including a comparison by orbital decomposition. In addition, we have studied the variation of the total energy with respect to the position of the As atoms. We have found that the TB total energies fit the LAPW values very well even for energies that we did not include in our fit.

II. COMPUTATIONAL DETAILS

The equilibrium structure of non-magnetic LaOFeAs is the AsCuSiZr structure²¹. This structure is tetragonal, space group P4/nmm, with eight atoms in the unit cell and lattice constants $a = 7.626$ Bohr and $c = 16.518$ Bohr. The Oxygen atoms occupy the (2a) Wyckoff positions, and Iron the (2b) positions. The La and As atoms occupy (2c) sites, with $z = 0.14154$ for La and 0.6512 for As. We used a regular, Γ -centered

$8 \times 8 \times 4$ k-point mesh, which results in 225 points in the irreducible part of the Brillouin zone. The LAPW basis functions were cut off at $RK_{max} = 8.5$, with approximately 1250 basis functions at each k-point. To help convergence we broadened the spectrum using a Fermi distribution at a temperature of 5 mRy.

As expected our LAPW energy bands and densities of states are basically identical to those published by Singh and Du⁹. We also performed 21 additional LAPW calculations by varying the above structural parameters a and z_{As} for the purpose of creating a first-principles total energy database to use in our TB calculations.

Our TB Hamiltonian was built following the NRL-TB method. We summarize below the basic equations of this scheme which is based on a Slater-Koster approach²² with two-center parameters.

Unlike the general NRL-TB method, where we include s , p , and d orbitals for each atom, here our basis set includes only the d orbitals for Fe and the p orbitals for As and O. All other contributions to the band structure, including the effects of La, are ignored as they have little weight in the region between the bottom of the As-O p bands and until well above the Fermi level. Since there are two Fe, As, and O in each unit cell of the structure, we end with a 22×22 matrix to diagonalize at each k-point. In addition, we limit ourselves to an orthogonal Hamiltonian, so we ignore the possible overlap hopping parameters.

Onsite Parameters In the NRL-TB, the onsite energies are determined by the interaction of an individual atom with its environment. In our study of LaOFeAs, however, we are considering at most small displacements of the atoms around the equilibrium positions. We therefore use a constant value for the onsite parameters. However, we recognize that the symmetry of the iron states allows the orbitals to have different onsite parameters. Accordingly, we chose four onsite parameters for Fe: one for the xz orbital, which will be equal to the yz parameter, and one each for the xy , $x^2 - y^2$ and $3z^2 - r^2$ orbitals. We also have one onsite parameter for the As p orbitals, and another for the O p orbitals, for a total of six independent onsite parameters, listed in Table I.

Hopping Parameters The usual spd Slater-Koster scheme has 10 two-center hopping parameters for like-atom interactions and 14 parameters for the interaction of two unlike atoms. Since we limit our system to Fe d and As/O p orbitals, we have only the following interactions:

Fe-Fe: $dd\sigma$, $dd\pi$, ddd

As-As (or O-O): $pp\sigma$, $pp\pi$

Fe-As (or Fe-O) (Fe atom first): $dp\sigma$, $dp\pi$

As-O: $pp\sigma$, $pp\pi$

for a total of 13 Slater-Koster parameters for each neighbor distance. As with the standard NRL-TB, these parameters depend only on the distance, R , between the two atoms, and are parametrized according to the formula

TABLE I: Onsite parameters for Fe-As-O, determined using the methods described in the text. All energies are in Rydbergs.

Atom	Orbital	Onsite
Fe	yz (zx)	0.51108
	xy	0.54617
	$x^2 - y^2$	0.54548
	$3z^2 - r^2$	0.5513
As	p	0.18566
O	p	0.39230

$$H_{\ell\ell'\mu}(R) = (a_{\ell\ell'\mu} + b_{\ell\ell'\mu}R + c_{\ell\ell'\mu}R^2) \exp(-d_{\ell\ell'\mu}^2 R) F(R), \quad (1)$$

where a, b, c and d are fitting parameters, and the cutoff function $F(R)$ has the form

$$F(R) = 1/\{1 + \exp[(R - R_0)/\ell]\}, R < R_0 \\ = 0, R > R_0. \quad (2)$$

In our fits we take $R = 14$ Bohr and $\ell = 0.5$.

The parameters in the above equations are determined by a least-squares fit to the LAPW eigenvalues at 225 k-points in the irreducible Brillouin zone. We have found that applying group theory to block-diagonalize the Hamiltonian at high symmetry points is essential for obtaining a good fit.

III. RESULTS

The onsite parameters determined from our fitting procedure are given in Table I. To make our results easier to compare to first-principles calculations we have rotated the Cartesian axis by 45° relative to the primitive vectors of the tetragonal unit cell, so that the lobes of the $x^2 - y^2$ Fe orbitals point to the nearest-neighbor Fe atoms.

In Table II we list the Slater-Koster hopping parameters generated by Eq. 1.

These parameters are designed to fit the 9^{th} to 21^{st} bands of our TB Hamiltonian to first principles results for three nearest neighbors of Fe-Fe, As-As, O-O, Fe-As, Fe-O, and As-O interaction. In Table III we show the RMS error per band for this fit, indicating the high quality of the fit to the LAPW eigenvalues. It should be noted that near the Fermi level which is in the vicinity of the 17^{th} and 18^{th} bands the deviation between LAPW and TB is on the average, including all the 225 k-points, 3mRy. At the high symmetry points such as at Γ , X and M the deviation is less than 1mRy, as can be seen in Fig. 1 which shows a comparison between LAPW and TB results.

The other TB papers¹¹⁻¹⁵ do not report the detailed quantitative information contained in our Table III, which makes it difficult to have a detailed comparison of TB models.

TABLE II: Slater-Koster hopping parameters generated by Eq. (1), as described in the text. Energy units are in Rydbergs, and distances are in Bohr.

Fe Fe	R	$dd\sigma$	$dd\pi$	$dd\delta$
	5.329	-0.02771	0.01001	0.00031
	7.626	0.00546	0.00029	0.00750
	10.784	0.00364	-0.00500	0.00008
As As	R	$pp\sigma$	$pp\pi$	
	7.350	0.05880	0.08276	
	7.626	0.06633	0.04262	
	10.784	0.01041	-0.05779	
O O	R	$pp\sigma$	$pp\pi$	
	5.392	0.01885	-0.00783	
	7.626	0.00939	-0.00534	
	10.784	0.00208	0.00085	
Fe As	R	$dp\sigma$	$dp\pi$	
	4.558	0.17916	0.00931	
	8.884	-0.00751	-0.02974	
	11.708	-0.00073	-0.00090	
Fe O	R	$dp\sigma$	$dp\pi$	
	8.259	-0.00319	-0.00338	
	9.863	0.00021	0.00240	
	11.241	-0.01449	0.00648	
As O	R	$pp\sigma$	$pp\pi$	
	6.909	0.00513	-0.02238	
	10.290	0.01562	-0.00206	
	11.412	0.00591	-0.00028	

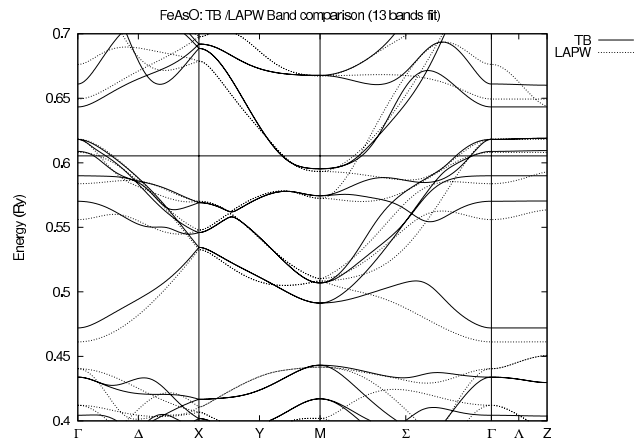


FIG. 1: A comparison of the LAPW (solid line) and tight-binding (dashed line) band structure for the bands near the Fermi level. The horizontal line at $y = 0.605$ Ry is the LAPW Fermi level.

The aforementioned 13 bands span an energy range from 0.4Ry to 0.75Ry as shown in Fig. 1. In this figure one can see that from 0.45 Ry where a gap is present to 0.70 Ry the fit is good and around the Fermi level (0.605Ry) the agreement between TB and LAPW is excellent; the energy bands clearly show holes around

TABLE III: RMS ERROR: per band for 225 k-points

Band	RMS Error (Ry)
9	0.008365
10	0.009243
11	0.011206
12	0.009935
13	0.011851
14	0.007552
15	0.005671
16	0.005491
17	0.002917
18	0.002912
19	0.007435
20	0.008658
21	0.012827
22	0.010253

the center of the Brillouin zone and electron pockets around the high symmetry point M. This suggests that the TB Fermi surface preserves all the characteristic features found in the first-principles calculations.

Our model also reproduces the LAPW Dirac cone, slightly shifted to the right and higher in energy by approximately 12.5 mRy (170 meV). There is a secondary erroneous crossing in the vicinity that is confusing to the eye. The TB model of Calderón *et al.*¹⁴ puts the Dirac cone at least 1 eV higher while Kuroki *et al.*¹¹ place it even higher. The model of Maier *et al.*¹⁵ seems to capture the Dirac cone (but may miss a Fermi crossing at Γ) as does that of Eschrig *et al.*¹³, though this is not a five-band model, but rather a downfolding technique which is in a different spirit than our approach. Of course none of the five-band models (nor any effective Fe-Fe only model) has the capability to turn individual (as compared to effective) hopping parameters on and off, as we do in a later section to understand the origin of the pseudogap.

In Fig. 2, we show a comparison between TB and LAPW densities of states. In Fig. 2 the total DOS are compared where one can see that TB matches well the two LAPW peaks below ε_F and the one peak above ε_F . The site decomposed DOS is also shown in Fig. 2 and shows very good agreement for the Fe d-states, and reasonable to good agreement for the As and O *p*-states. One can conclude that the TB produces reliable results not only for the eigenvalue spectrum but also for the eigenvectors.

The orbitally decomposed DOS are also in at least semi-quantitative agreement between LAPW and TB results. Note that since the LAPW angular-momentum components of the DOS are projections inside the muffin-tin spheres, an exact comparison cannot be made. Still, the TB is a powerful tool in explaining features of the DOS that cannot be addressed by the first-principles calculations. For example, we can trace down the origin of the the so-called pseudogap above ε_F shown in Fig. 2.

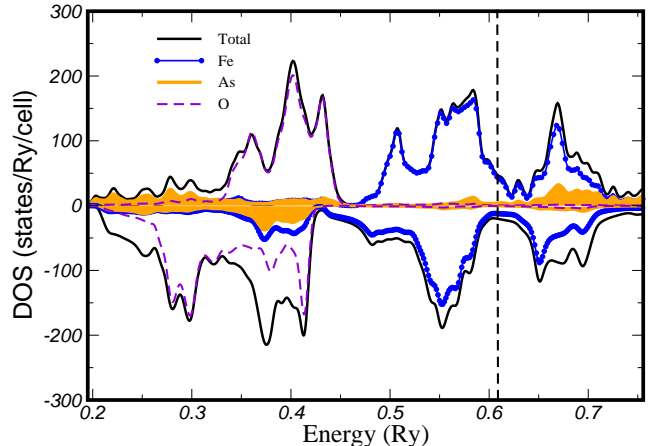


FIG. 2: (color online) Comparison of the LAPW (lower half) and TB (upper half) DOS. Site decomposition for Fe, As, and O is also shown.

Since the local environment of the Fe atom is tetragonal (distorted to some degree in most 1111 type compounds), and given that the strongest hopping parameter is the Fe-As $dp\sigma$, as seen in Table II, one might expect to see a gap or pseudogap between a lower e_g doublet and an upper t_{2g} triplet, commensurate with the local symmetry. However, in reality the gap occurs between a lower peak in the DOS containing three states per Fe (six total) and an upper peak containing two states per Fe (four total), *i.e.* the reverse of the naive ligand field (or crystal field) expectation (this can be seen in Fig. 2 in the Fe part of the spectrum). Here we use our TB model to eliminate hoppings one by one and trace down the origin of the pseudogap.

First we turn off all but the Fe-As nearest neighbor hoppings and indeed find a lower doublet and upper triplet, as must be the case (see Fig. 3). The splitting between triplet states, and to a lesser degree the doublet states, is due to the imperfect tetrahedron.

Next, we eliminate all Fe-As hopping, but allow hopping between the two distinct Fe (these are nearest Fe neighbors) in the unit cell. As can be seen in Fig. 4, this has the effect of creating bonding/anti-bonding complexes within each orbital designation. Interestingly, the $xz + yz$ orbitals do not split at all, remaining as a single peak, while the most strongly split orbital is xy . Already, something like a pseudogap can be seen to be forming around 0.57 Ry, with a spectral distribution quite different from the ligand field gap distribution in Fig. 3.

Finally, we allow *all* Fe-As hoppings, but remove direct Fe-Fe hopping. This scenario accounts for interaction between the two Fe sites in the unit cell via As. In Fig. 5, a bonding/anti-bonding splitting again occurs in most of the orbitals with the strength of the splitting considerably stronger than that initiated by Fe-Fe direct hopping.

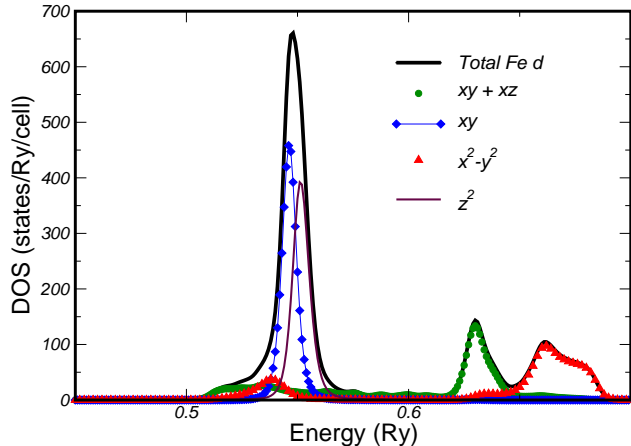


FIG. 3: (color online) The DOS with only nearest neighbor Fe-As hoppings included. The expected ligand field splitting corresponding to the tetragonal environment of the Fe atom is clearly visible.

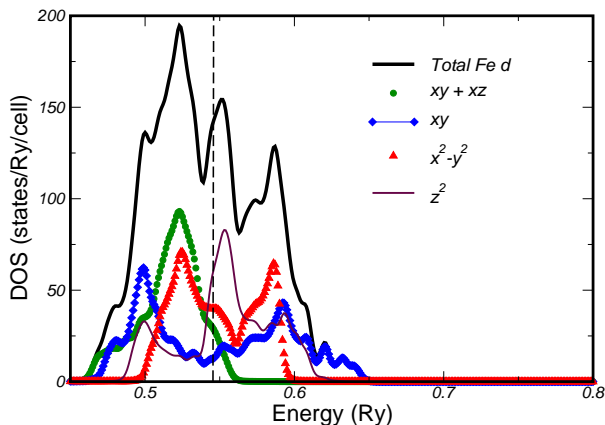


FIG. 4: (color online) The DOS with all hoppings eliminated except direct hopping between Fe atoms. Most of the orbitals split into bonding/anti-bonding combinations with only the $xz + yz$ combination remaining as a single peak.

In this case the $xy + xz$ orbital does undergo splitting, but the z^2 and xy orbitals do not. A fairly strong pseudogap emerges with the majority of the weight in the lower complex. Note that there are still significant differences between the DOS in Fig. 5 and the full TB model DOS in Fig. 2. This underlines the importance of direct Fe-Fe hopping.

Combining the information from all three reduced hopping diagrams, we can understand how the pseudogap forms. It is the result of a combination of strong and weak bonding/anti-bonding splitting of the orbitals, due

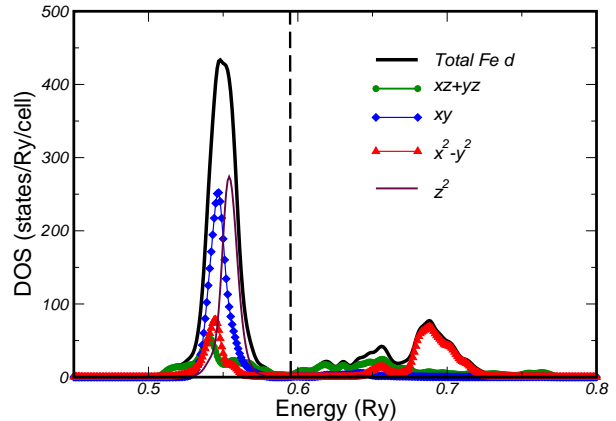


FIG. 5: (color online) The DOS including all Fe-As hoppings, but without any direct Fe-Fe hopping. The z^2 and xy orbitals remain unsplit, while all other orbitals show rather strong bonding/anti-bonding peak separations.

to the two distinct Fe atoms in the unit cell. Hopping occurs both via As and directly between Fe atoms (further hoppings also surely contribute somewhat). In Fig. 6, we show how very strong splitting of the t_{2g} -triplet derived states coupled with weaker splitting of the e_g doublet-derived states results in the calculated pseudogap. The $xz + yz$, $x^2 - y^2$ orbitals split strongly into two peaks per orbital, forming an upper complex of three states and a lower one also of three states. The xy orbital has a weaker splitting, but strong enough still to place one state in the upper complex and one in the lower. Not surprisingly, the z^2 orbital, which is pointed mainly out-of-plane, has the weakest splitting such that both the bonding and anti-bonding peaks remain in the lower complex. Thus, there are six states in the lower complex and four in the upper. Note that the actual splitting of the xy state is somewhat more complicated than the simple bonding/anti-bonding schematic suggests. This simply mirrors the fact that the DOS itself is not composed of two simple peaks of precisely six and four states each, but rather has some secondary peak structures. In addition, all of the states are broadened into bands which, along with strict symmetry requirements¹³ cause finite overlap between the upper and lower complexes and give rise to a pseudogap rather than a full gap. By turning off specific hoppings, we have elucidated from an atomic orbital point of view, the mechanism that gives rise to the pseudogap. It requires both direct Fe-Fe interaction *and* interaction via the intermediate As.

The second fit that we performed has the objective to fit the volume and the As position variations of the total energy. The height of the As ion has strong effects on the electronic structure and magnetism and may even be able to switch the pairing symmetry^{11,23,24}. For this purpose we run 21 separate LAPW calculations to fit in our TB

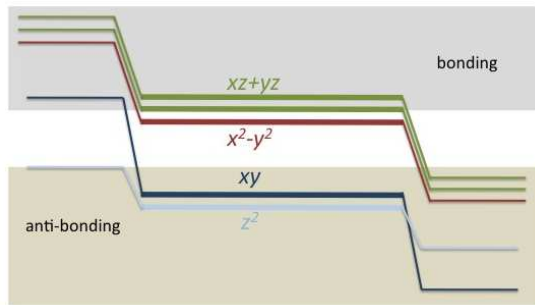


FIG. 6: (color online) A schematic illustrating the origin of the pseudogap. Each of the original five orbitals is doubly degenerate (one set coming from each Fe in the unit cell). The $xz + yz$, $x^2 - y^2$, and xy orbitals bonding and anti-bond with sufficient strength to form upper and lower complexes, designated by the two shaded regions. The z^2 orbital has a small splitting, but both peaks remain in the lower complex. The pseudogap and Fermi energy lie between the upper (anti-bonding only) and lower (mostly bonding) complexes.

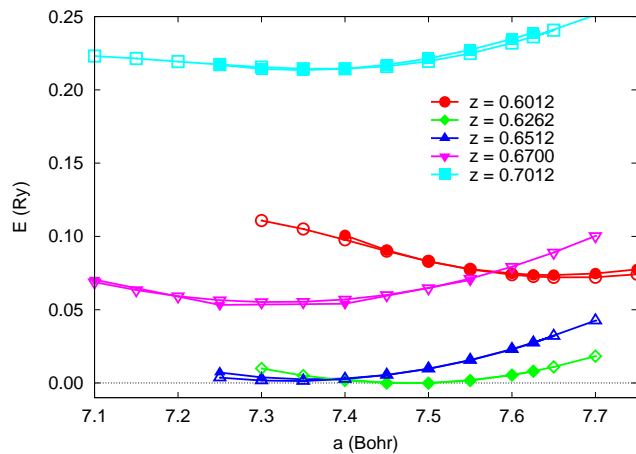


FIG. 7: (color online) The total energy curves generated by TB fits (open symbols) to LAPW data (solid symbols) for various values of the As height above the Fe plane and planar lattice constant, for fixed lattice constant $c = 16.4$ *a.u.*

scheme the total energy. In this calculation we fitted all the 22 energy bands that correspond to our Fe(d)-As(p)-O(p) TB Hamiltonian. This fit does not give the excellent fit to the LAPW Fermi surface that we found in the first fit. However, it fits the 21 LAPW total energies perfectly with an RMS error of 0.0004 Ry. In Fig. 7 we show the total energy results of this fit. We used these TB parameters to calculate total energies outside our database and compared with independent LAPW results not included in the fit and found very good agreement. Using these results we found the lattice equilibrium parameters to be $a=7.4$ *a.u.*, $c=16.4$ *a.u.* and As position $z=0.64$ (giving 113.5° as the As-Fe-As angle), in reasonable agreement with the experimental values.

IV. CONCLUSIONS

We report TB results on LaOFeAs obtained by the NRL-TB method via a fit to LAPW eigenvalues and total energies. Two TB parametrizations were performed: the first aims at reproducing the energy bands in an energy range from 2.7 eV below to 0.8 eV above ε_F with superior accuracy around ε_F . From this parametrization an analysis of the orbital-decomposed DOS shows that the mechanism which creates the pseudogap above ε_F comes from a direct Fe-Fe interaction and from an Fe-Fe interaction through the intermediate As atom. In our second TB parametrization we focus on the energetics of the LaOFeAs system finding a TB Hamiltonian that fits the LAPW total energies as a function of volume and As position very well. We propose that this TB Hamiltonian will be very useful in carrying out many-body theory with a more realistic Hamiltonian than those employed previously containing just the d-iron orbitals.

Acknowledgments

We thank Igor Mazin for useful discussion. The work at GMU is supported by ONR grant No: N000140911025, and the work at NRL is supported by the Office of Naval Research.

¹ Y. Kamihara, T. Watanabe, and J. M. Hirano and H. Hosono, *J. Am. Chem. Soc.* **130**, 3296 (2008).
² Z.-A. Ren, W. Lu, J. Yang, W. Yi, X.-L. Shen, C. Zheng, G.-C. Che, X.-L. Dong, L.-L. Ling, F. Zhou, et al., *Chin. Phys. Lett.* **25**, 2215 (2008).
³ C. de la Cruz, Q. Huang, J. Lynn, J. Li, W. Ratcliff, J. Zarestky, H. Mook, G. Chen, J. Luo, N. Wang, et al., *Nature* **453**, 899 (2008).
⁴ H. Wen, G. Mu, L. Fang, H. Yang, and X. Zhu, *Europhys. Lett.* **82**, 17009 (2008).
⁵ G. Cao, S. Jiang, X. Lin, C. Wang, Y. Li, Z. Ren, Q. Tao, J. Dai, Z. Xu, and F.-C. Zhang, *Phys. Rev. B* **79**, 174505

(2009).
⁶ Y. Kamihara, H. Hiramatsu, M. Hirano, R. Kawamura, H. Yanagi, and T. Kamiya, *J. Am. Chem. Soc.* **128**, 10012 (2006).
⁷ P. Hohenberg and W. Kohn, *Phys. Rev.* **136**, B864 (1964).
⁸ W. Kohn and L. J. Sham, *Phys. Rev.* **140**, A1133 (1965).
⁹ D. Singh and M.-H. Du, *Phys. Rev. Lett.* **100**, 237003 (2008).
¹⁰ T. Yildirim, *Phys. Rev. Lett.* **101**, 057010 (2008).
¹¹ K. Kuroki, H. Usui, S. Onari, R. Arita, and H. Aoki, *Phys. Rev. B* **79**, 224511 (2009).
¹² S. M. E. Manousakis, J. Ren and E. Kaxiras, *Phys. Rev.*

- B **78**, 205112 (2008).
- ¹³ H. Eschrig and K. Koepnik, Phys. Rev. B. **80**, 104503 (2009).
- ¹⁴ M. J. Calderón, B. Valenzuela, and E. Bascones, Phys. Rev. B **80**, 094531 (2009).
- ¹⁵ S. Graser, T. A. Maier, P. J. Hirschfeld, and D. J. Scalapino, New. J. Phys. **11**, 025016 (2009).
- ¹⁶ M. Mehl and D. Papaconstantopoulos, Phys. Rev. B **54**, 4519 (1996).
- ¹⁷ M. Johannes, D. Papaconstantopoulos, D. Singh, and M. Mehl, Europhys. Lett. **68**, 433 (2004).
- ¹⁸ D. D. Koelling and B. N. Harmon, J. Phys. Chem. **10**, 3107 (1977).
- ¹⁹ S.-H. Wei and H. Krakauer, Phys. Rev. Lett. **55**, 1200 (1985).
- ²⁰ D. Singh, H. Krakauer, and C. S. Wang, Phys. Rev. B **34**, 8391 (1986).
- ²¹ V. Johnson and W. Jeitschko, J. Solid State Chem. **11**, 161 (1974).
- ²² J. C. Slater and G. F. Koster, Phys. Rev. **94**, 1498 (1954).
- ²³ Z. Yin and W. Pickett, Phys. Rev. Lett. **101**, 047001 (2008).
- ²⁴ I. Mazin, M. Johannes, L. Boeri, K. Koepnik, and D. Singh, Phys. Rev. B. **78**, 085104 (2008).